Available online at www.sciencedirect.com
ScienceDirect
IFAC PapersOnLine 51-2 (2018) 97–102

Development of a test system for identification of turbine dynamics using the dc power flow

Sigurd Hofsmo Jakobsen * Kjetil Uhlen *

* Department of Electric Power Engineering, Norwegian University of Science and Technology, Trondheim, Norway, sigurd.h.jakobsen@ntnu.no

Abstract: Recent concerns about the frequency quality in the Nordic power system has lead to increased research on hydro turbine governors. Among this research is the use of system identification methods. However, there has been no theoretical validation of the approaches used. To be able to do a theoretical validation a simple test system is needed. In this paper it is described how one can develop such a simple test system using the dc power flow equations. In addition the system is tuned according to parameters given by recent studies to have a realistic frequency response.

1. INTRODUCTION

In the power system there is a strong coupling between active power and frequency. The frequency dynamics are mostly determined by the turbine governors of the large synchronous machines in the power system. Studying the dynamics of these therefore makes sense with respect to analysing frequency quality problems.

Different approaches have been proposed for identifying hydro turbine dynamics. For instance one could identify the dynamics by exciting the system externally and using measurements at the plant as in Saarinen et al. (2015). Another approach is to use Phasor measurement units (PMUs) and assume that the power system itself sufficiently excites the turbine dynamics as in Sigurd Hofsmo Jakobsen and Kjetil Uhlen (2017); Dinh Thuc Duong et al. (2016); Mogharbel et al. (2015). Common for the approaches using PMUs is that they don't consider how the input and output signals of the identification are related through the power system. This is an important aspect to consider since the input to the identification will be a function of the output to the identification problem. It is therefore essential to analyse that the input signal will be sufficiently exciting. To do this the analytical relation between the power and frequency at the generator buses have to be considered.

A simple model often used in the literature for studying generators connected to a larger power system is the single machine infinite bus (SMIB) system. This system can be found in for instance the text book Kundur et al. (1994). A SMIB system consists of a generator, an infinite bus and line connecting them. The infinite bus is characterised by having, constant voltage, voltage angle and frequency and is meant to represent a large power system. One famous example is the Heffron-Phillips system Heffron and Phillips (1952), that was proposed for studying voltage regulators. For our purpose voltages and reactive power are not important and we will therefore use a dc power flow equation with constant voltages. The use of a dc power flow will simplify the expressions. Furthermore, it also has many advantages when it comes to computational speed and convergence Stott et al. (2009).Although, a dc power flow have some shortcomings when it comes to accuracy, it is believed to be acceptable for studying low frequency dynamics. However, care should be taken as voltage control has significant influence on electromechanical dynamics.

The proposed test system can be seen as an extension of a classical SMIB system. Opposed to a classical SMIB system there will be no infinite bus, rather an aggregated generator. Furthermore, a load bus will be included. The load bus is important to include since the stochastic loads are what excites the system. In addition the frequency dependent load also influences the power and should be included. It is important to notice that the modelling techniques in this paper are all standard power system modeling techniques. The novelty lies in applying these techniques to create a small test system that can be used for easily analysing identification problems including power and frequency. In addition the approach used for developing the test system can be applied for analysing frequency control strategies and power system frequency response.

The paper will be organized such that modelling of frequency dynamics are presented in Section 2. How the different elements are connected together to form a system is described in Section 3. To show the performance of the methodology some simulation results are presented in Section 4 before the conclusions in Section 5.

2. FREQUENCY DYNAMICS

One of the main task of the power system is to maintain a constant frequency Kundur et al. (1994). This is achieved by constantly balancing the power consumed and the power produced in the system, a process often referred to as frequency control. Typically one talks about three levels of frequency control. The frequency containment control is the fastest acting control. It is a distributed controller

2405-8963 © 2018, IFAC (International Federation of Automatic Control) Hosting by Elsevier Ltd. All rights reserved.
Peer review under responsibility of International Federation of Automatic Control.
10.1016/j.ifacol.2018.03.017

situated at most turbines. The next level of control is the frequency restoration control, which is responsible for bringing the frequency back to its nominal value and to bring tie line powers back to their scheduled values. This is a slower centralized control. The last level is the replacement reserves. These are standby reserves that should be activated to ensure that the system has enough restoration and containment reserves. In addition the inertia in the synchronous machines and rotating loads influence the frequency of the power system, this effect is often referred to as the inertial response.

In this section the elements relevant in the frequency range of the inertial response and the frequency containment response will be presented.

2.1 The swing equation

The inertial response of the power system is related to the energy stored in the rotating mass of the turbine and generator, which rotates at a speed synchronous to the grid frequency, and can be mathematical described as:

$$\begin{aligned}\dot{\theta}_m &= \omega_m \\ J\dot{\omega}_m + D_d\omega_m &= T_m - T_e\end{aligned} \tag{1}$$

where:

θ_m: is the angular position of the machine's rotor,
ω_m: is the angular velocity of the machine's rotor,
J: is the total moment of inertia of the machine,
D_d: is the damping torque,
T_m: is the mechanical torque of the turbine and,
T_e: is the torque of the electrical field in the machine.

The equation is well known and described in most standard text books for power systems such as for instance Machowski et al. (2008) and Kundur et al. (1994). Since power is torque times the angular velocity (1) can be written as:

$$J\dot{\omega}_m + D_d\omega_m = \frac{P_m}{\omega_m} - \frac{P_e}{\omega_m} \tag{2}$$

To simplify the expression we multiply with the synchronous machine speed ω_{sm} and the assumption $\omega_m \approx \omega_{sm}$ is used. This is a common assumption since the machine speeds normally not deviate a lot from synchronous speed even during disturbances.

$$\omega_{sm}J\dot{\omega}_m + \omega_{sm}D_d\omega_m = P_m - P_e \tag{3}$$

It is common to express the swing equation in terms of the inertia constant defined as follows:

$$H = \frac{J\omega_{sm}^2}{2S} \tag{4}$$

where S is the rating of the machine. We also define

$$D_m = \omega_{sm}D_d \tag{5}$$

By inserting the new constants into (3) we get.

$$\frac{2HS}{\omega_{sm}}\dot{\omega}_m + \omega_m D_m = P_m - P_e \tag{6}$$

Since we are mostly interested in the electrical angular speed ω the following relation between the electrical, mechanical angular speed and number of poles p is used:

$$\omega_m = \frac{\omega}{p/2} \tag{7}$$

Inserting (7) into (6) gives:

$$\frac{2HS}{\omega_s}\dot{\omega} + \frac{2}{p}\omega D_m = P_m - P_e \tag{8}$$

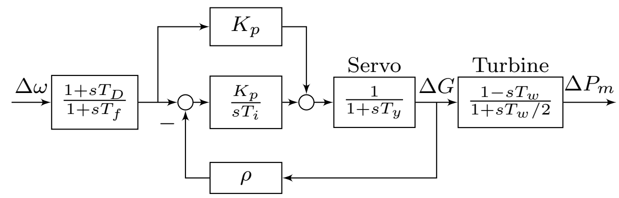

Fig. 1. Hydro turbine governor and turbine

Notice that ω_s is the electrical synchronous speed. In our notation the subscript m is dropped when going from mechanical to electrical values. Now we divide (8) by the machine rating to get the powers in per unit.

$$\frac{2H}{\omega_s}\dot{\omega} + \frac{2}{Sp}\omega D_m = P_m^{pu} - P_e^{pu} \tag{9}$$

From now on if not stated otherwise the powers will be in per unit. We also define:

$$K_d = \frac{2}{p}\frac{D_m}{S} \tag{10}$$

By using this the final version of the swing equation is obtained

$$\frac{2H}{\omega_s}\dot{\omega} + K_d\omega = P_m - P_e \tag{11}$$

2.2 Frequency containment control

After the inertial response the primary frequency control or frequency containment control takes over. It is a local controller at most turbines, which governs how much a turbine should change its power output given a frequency deviation. An example on how this controller could be implemented and it's relation to the turbine dynamics are depicted in Fig. 1. The signals in the figure are as follows:

ΔP_m: is the change in turbine mechanical power,
ΔG: is the change in the gate position, and
$\Delta\omega$: is the speed deviation

The parameters in Fig. 1 and the values used are given in TABLE 1. Fig. 1 depicts a governor and its connection

Table 1. Hydro turbine governor parameters

Variable	Explanation	Value
T_D	Derivative time	0
T_f	Low pass filter time constant	0
K_p	Controller gain	1.5
T_i	Integral time	9.1s
ρ	Droop	0.1
T_y	Servo time constant	0.2s
T_w	Water starting time	1.01s

to the turbine. In between the PID regulator is a servo controlling the gate, which normally is modeled as a first order lag Working Group on Prime Mover and Energy Supply Models for System Dynamic Performance Studies (1992). The constant ρ in the feedback determines how much the power output of the generator should change given a frequency deviation and is referred to as the droop. The feedback could also be from the measured power. In this case when it's from the measured gate opening a look up table relating gate opening to produced mechanical power is used to determine the gate opening.

Other more detailed models commonly used are described in Working Group on Prime Mover and Energy Supply Models for System Dynamic Performance Studies (1992) and a review of what can be found in the literature is given in Kishor et al. (2007).

2.3 Frequency dependent loads

In addition to the inertial response of the system's generators and the primary frequency response there are also frequency dependent loads. The equation used for describing the load behavior is as follows:

$$\Delta P_{load} = \Delta P_f + \Delta P_s \tag{12}$$

where:

ΔP_f: is frequency dependent part of the load
ΔP_s: is the stochastic part of the load assumed to be the integral of white noise.

For the frequency dependent part the following model will be used:

$$\Delta P_f = \frac{1}{D}\Delta f + \frac{W_0}{f_0}\Delta \dot{f} \tag{13}$$

where:

ΔP_f : is the change in electrical power due to frequency dependent loads,
D : is a constant,
W_0 : is the energy stored in the rotating masses at the linearization point and,
f_0 : is the frequency at the linearization point.

On the load bus the swing equation cannot be used for calculating the frequency. The two main approaches for calculating the frequency at such buses are to use a weighted sum of the generator speeds or the derivative of the voltage angle at the bus Hsu et al. (1998). In this study the load bus frequency will be calculated as a weighted sum of the generator speeds.

$$f_L = \frac{\sum_{i=1}^{n_g} H_i\omega_i}{2\pi\sum_{i=1}^{n_g} H_i} \tag{14}$$

where:

f_L: is the load frequency,
ω_i: is the speed at generator bus i,
n_g: is the number of generators in the system,
H_i: is the inertia constant of bus i.

Other approaches for modelling frequency at load buses exist such as the recent frequency divider equation Milano and Ortega (2017). This approach could be useful if one need to model spatial variation of the frequency. As it gives an algebraic expression for the frequency at load buses dependent on the system reactances.

2.4 Model of an aggregated generator

A model for an aggregated generator consisting of N_g generators will also be derived. We will refer to the set of generators as Ω_g. The derivation shown here is based on Göran Andersson (2012). We start with (11) and multiply it with S_i, which is the rating of generator i. Furthermore, we use that $\omega = \dot{\theta}$.

$$\frac{2H_iS_i}{\omega_s}\dot{\omega}_i + K_{di}S_i\omega_i = P_{mi} - P_{ei} \tag{15}$$

Now we sum over (15) for all the generators on the bus:

$$2\sum_{i\in\Omega_g}(\frac{H_iS_i}{\omega_s}\dot{\omega}_i + K_{di}S_i\omega_i) = \sum_{i\in\Omega_g}(P_{mi} - P_{ei}) \tag{16}$$

To simplify (16) we define the following quantities:

$$\omega = \frac{\sum_{i\in\Omega_g} H_i\omega_i}{\sum_{i\in\Omega_g} H_i} \tag{17}$$

$$S = \sum_{i\in\Omega_g} S_i \tag{18}$$

$$H = \frac{\sum_{i\in\Omega_g} H_iS_i}{\sum_{i\in\Omega_g} S_i} \tag{19}$$

$$K_d = \frac{\sum_{i\in\Omega_g} K_{di}S_i}{\sum_{i\in\Omega_g} S_i} \tag{20}$$

$$P_m = \sum_{i\in\Omega_g} P_{mi} \tag{21}$$

$$P_e = \sum_{i\in\Omega_g} P_{ei} \tag{22}$$

We can now write the swing equation for the bus as

$$\frac{2HS}{\omega_s}\dot{\omega} + K_dS\omega = P_m - P_e \tag{23}$$

In addition to aggregating the swing equation the turbine, governor and reactances also have to be aggregated. The turbine and governor can be represented by a transfer function $G_t(s)$. At the bus there will be N_g of these transfer functions all contributing to the mechanical power.

$$P_m = \sum_{i\in\Omega_g} G_{t2} \tag{24}$$

For the reactances of the machines at the aggregated bus it is reasonable to assume them to be connected in parallel, which gives the following expression:

$$\frac{1}{x'_d} = \sum_{i\in\Omega_g}\frac{1}{x'_{di}} \tag{25}$$

3. THE DC POWER FLOW

In this section the version of the dc power flow used for this paper is presented. A description on how one can interface the dc power flow with the necessary power system components is also provided.

3.1 Grid interface of the synchronous machine

Before moving on to describe the dc power flow we will first introduce how the models presented in the previous section can be interfaced with the dc power flow. In the literature one can find that it is normal to represent synchronous generators as a source behind an impedance Kundur et al. (1994). The impedance is also dominated by the reactance, hence, we will model it as a reactance. Furthermore, the reactance will be dependent on the transients such that the value will be larger for faster transients. Typically, one will divide the analysis into a sub-transient, transient and a steady state period. In our analysis we will use the transient reactance. Schematically this representation of a synchronous generator is depicted in Fig. 2. In other words the generator will be modelled as a source behind its transient reactance as seen from a power flow perspective.

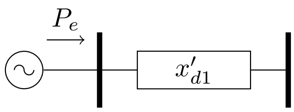

Fig. 2. Generator behind a transient reactance

3.2 DC power flow

The power flowing on the lines in a power system is related to the power injections at the buses through the power flow equations. Below the power flow equation for active power is written neglecting the terms related to ohmic losses and shunt elements. Basically the equation tells us that the power injected into a bus equals all the powers flowing into it from adjacent lines.

$$P_k = U_k \sum_{m \in \Omega_k} U_m x_{km}^{-1} \sin\theta_{km} \tag{26}$$

where:

P_k**:** is the power injection at node k,
θ_{km}**:** is the voltage angle difference between node k and m,
x_{km}**:** is the reactance between node k and m,
Ω_k**:** is the buses adjacent to bus k.
U_k**:** is the voltage at bus k.
U_m**:** is the voltage at bus m.

In real power systems the voltages are normally close to $1(p.u.)$ and the angles are small. Using these observations the DC power flow approximation is written as follows:

$$P_k \approx \sum_{m \in \Omega_k} x_{km}^{-1} \theta_{km} \tag{27}$$

Written on matrix form this becomes:

$$\mathbf{P} = \mathbf{Y}\theta \tag{28}$$

where:

P: is the vector of power injections,
Y: is the nodal admittance matrix,
θ**:** is the vector of voltage bus angles.

Since the angles at the load buses are unknown we split the admittance matrix into submatrices to derive an expression for the power injection at the generator buses.

$$\begin{bmatrix} \mathbf{P}_e \\ \mathbf{P}_l \end{bmatrix} = \begin{bmatrix} \mathbf{Y}_{11} & \mathbf{Y}_{12} \\ \mathbf{Y}_{21} & \mathbf{Y}_{22} \end{bmatrix} \begin{bmatrix} \theta_e \\ \theta_l \end{bmatrix} \tag{29}$$

where:

$\mathbf{P}_e$**:** is the power injection at the generator nodes
$\mathbf{P}_l$**:** is the power injection at the loads
θ_e**:** is the voltage angle at the generator nodes
θ_l**:** is the voltage angle at the load nodes

The angle of the load buses can now be calculated as:

$$\theta_l = \mathbf{Y}_{22}^{-1}(\mathbf{P}_l - \mathbf{Y}_{21}\theta_e) \tag{30}$$

Finally the power injections at the generator buses are:

$$\mathbf{P}_e = \mathbf{Y}_{11}\theta_e + \mathbf{Y}_{12}\theta_l \tag{31}$$

If one is not interested in the angle of the load buses and are only interested in the injected power at the generator node it can be convenient to substitute (30) into (31) and rearrange to obtain.

$$\mathbf{P}_e = \begin{bmatrix} \mathbf{Y}_{11} - \mathbf{Y}_{12}\mathbf{Y}_{22}^{-1}\mathbf{Y}_{21} & \mathbf{Y}_{12}\mathbf{Y}_{22}^{-1} \end{bmatrix} \begin{bmatrix} \theta_e \\ \mathbf{P}_l \end{bmatrix} \tag{32}$$

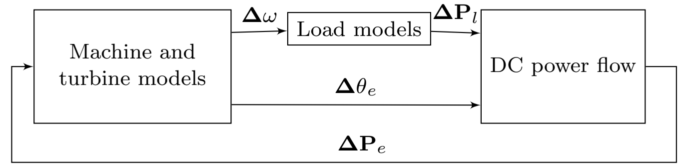

Fig. 3. Conceptual connection between device models and DC power flow

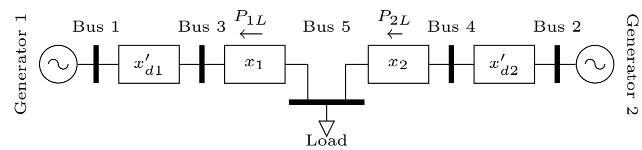

Fig. 4. System set up

From (32) one can see that the input needed to the DC power flow are the change in generator angles and the change in the demand. The change in the generator angles are easily calculated as the integral of the generator speeds. Furthermore, the calculated injected power at the generators are input to the swing equation. This means that the machine models, loads and dc power flow equation together form a feedback loop, as depicted in Fig. 3.

4. SIMULATION RESULTS

In this section simulation results from the test system is presented and compared to PMU data. The PMU data was collected using a PMU installed close to a generator in the Nordic power system.

To study the identifiability of turbines using PMU measurement the system depicted in 4 is proposed. It consists of a generator at bus 1, a load at bus 5 and an aggregated generator at bus 2. At bus 2 it is assumed to be 10 generators that have exactly the same parameters. If one increases the number of generators at bus the system will gradually go towards a single machine infinite bus system. The idea behind the layout of the system is that bus 1 represents the bus where one has PMU measurements and will attempt the identification, bus 2 represents the rest of the generators, and bus 5 represents the loads in the system. The block diagram is depicted in 4. In addition to what have been described earlier the diagram also contains blocks for changing between the different per unit systems and also for going from frequency to radians. The parameters used are given in 2. In the table base voltages for the machines and transmission system are also reported. These are used for converting the sub transient reactances to the same base as the transmission grid. A block diagram representation of the system is depicted in Fig. 5. The constants denoted K in the figure corresponds to the elements of the matrix in (32).

To get a realistic frequency response the values reported in the paper Saarinen et al. (2016) were used for tuning the governor.

To check whether or not the system response is reasonable a random load with a standard deviation of 0.025 was simulated. This signal was sent through an integrator to represent the load as the integral of white noise. This is a commonly used method for representing stochastic loads in

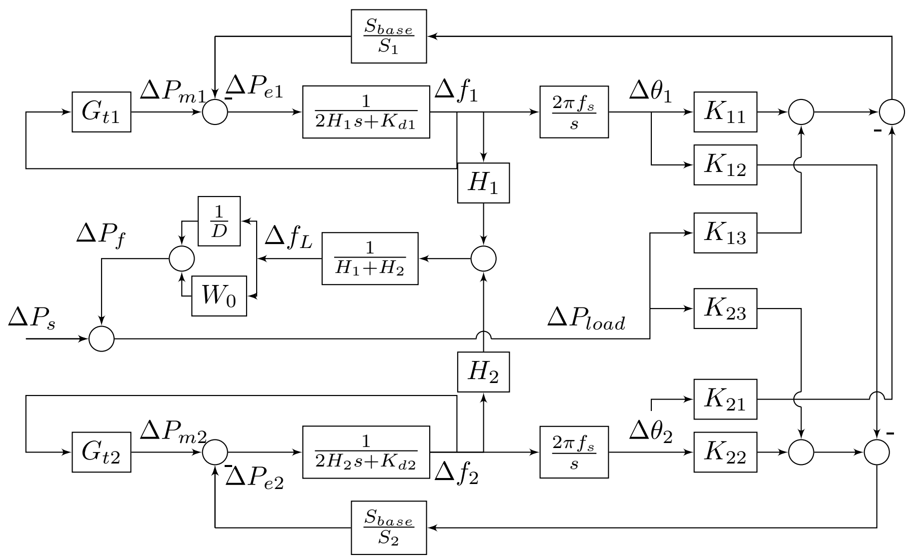

Fig. 5. Block diagram of Fig. 4

the power system Perić and Vanfretti (2014). The results from this simulation was used to plot the power spectral density of the simulated frequency against a measured signal. The result of this is shown in Fig. 6. As one can see it is a reasonably good match.

In Fig. 7 the system frequency's response to a one per unit load step is plotted. One can see that the change in frequency is less than expected given the applied step, if one assumed the change to be directly proportional to the droop of the governors. However, since the damping K_{d2} is quite large this also contributes to the final change in the frequency deviation. Since the model used is quite simple some of the damping provided by for instance the damper windings have to be included in the model and it is common to choose the damping factors larger to overcome this problem. To obtain a steady state change directly proportional to the droop one could choose to model the damping as only acting while the frequency is changing as in Andersen (2016).

Table 2. The parameters used for Fig. 5

Variable	Explanation	Value	
S_1	Machine 1 base power	$300MW$	-
S_2	Machine 2 base power	$3GW$	-
S_{base}	System base power	$3.3GW$	-
U_{base}	Base voltage for the transmission system	$400kV$	-
U_M	base voltage for the machines	$20kV$	-
D	Proportional load frequency dependency	50	S_{base}
W_0	Energy stored in rotating loads	0.01	S_{base}
H_1	Generator 1 inertia constant	$9.68s$	
H_2	Generator 2 inertia constant	$96.8s$	
K_{d1}	Damping constant	0.5	-
k_{d2}	Damping constant	5	-
x_1	Reactance between bus 3 and 5	5	S_{base}
x_2	Reactance between bus 4 and 5	5	S_{base}
x_{d1}	Sub transient reactance generator 1	0.15	S_1
x_{d2}	Sub transient reactance generator 2	0.15	S_1

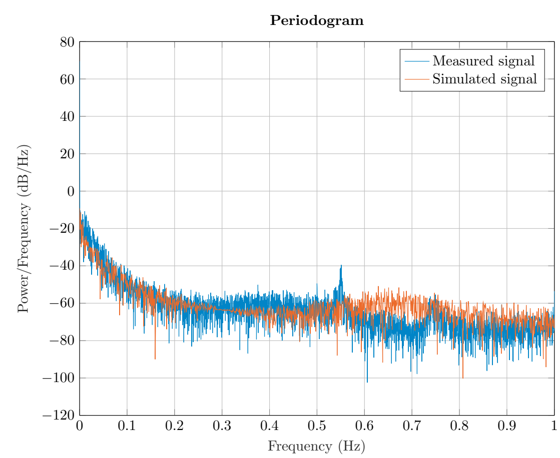

Fig. 6. Power spectrum density of measured system frequency and simulated frequency

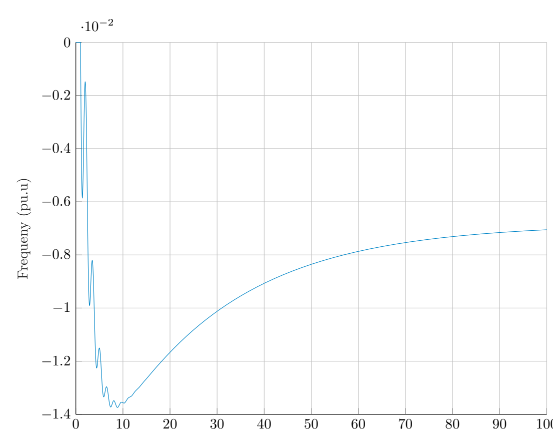

Fig. 7. Frequency response to a 1(p.u.) load step

A plot of the powers flowing on the lines is also given in Fig. 8. As one could expect most of the load change is being compensated by the larger generator at bus 2.

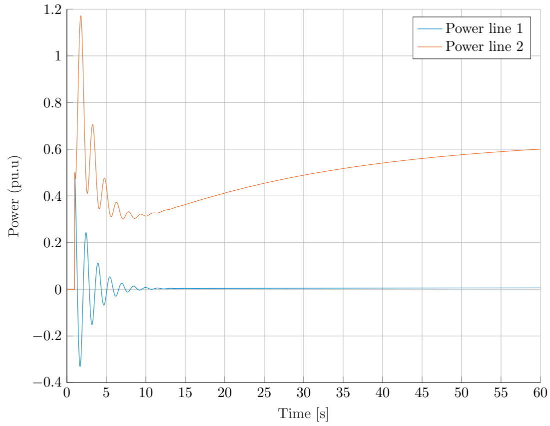

Fig. 8. Generator power response to a 1(p.u.) load step

5. CONCLUSIONS

In the paper it has been shown how one can create a simple test system for studying frequency control. The system shows similar frequency dynamics to the real power system when tuned with parameters from a recent study and should be suited for studying identification of turbine and turbine governor dynamics. Furthermore, the methodology can easily be adapted for other frequency studies. However, if one want a more correct representation of the system's droop characteristic another model of the damping will have to be implemented.

ACKNOWLEDGEMENTS

The work presented in this paper was carried out in the project OperaGrid funded by the Norwegian research council. In addition the ELECTRA IRP FP7 project funded the research exchange between NTNU and Ampere Lab.

REFERENCES

Andersen, K.G. (2016). *Area Based Secondary Frequency Control in the Nordic Power System*. Ph.D. thesis, Norwegian University of Science and Technology.

Dinh Thuc Duong, Kjetil Uhlen, Stig Løvlund, and Erik Alexander Jansson (2016). Estimation of Hydro Turbine-Governor's Transfer Function from PMU Measurements. IEEE, Boston.

Göran Andersson (2012). *Dynamics and Control of Electric Power Systems*.

Heffron, W.G. and Phillips, R.A. (1952). Effect of a Modern Amplidyne Voltage Regulator on Underexcited Operation of Large Turbine Generators [includes discussion]. *Transactions of the American Institute of Electrical Engineers. Part III: Power Apparatus and Systems*, 71(1). doi:10.1109/AIEEPAS.1952.4498530.

Hsu, C.S., Chen, M.S., and Lee, W.J. (1998). Approach for bus frequency estimating in power system simulations. *Transmission and Distribution IEE Proceedings - Generation*, 145(4), 431–435. doi:10.1049/ip-gtd:19982028.

Kishor, N., Saini, R.P., and Singh, S.P. (2007). A review on hydropower plant models and control. *Renewable and Sustainable Energy Reviews*, 11(5), 776–796. doi: 10.1016/j.rser.2005.06.003.

Kundur, P., Balu, N.J., and Lauby, M.G. (1994). *Power system stability and control*, volume 7. McGraw-hill New York.

Machowski, J., Bialek, J.W., and Bumby, J.R. (2008). *Power System Dynamics : Stability and Control*, volume 2nd ed. Wiley, Chichester, U.K.

Milano, F. and Ortega, A. (2017). Frequency Divider. *IEEE Transactions on Power Systems*, 32(2), 1493–1501. doi:10.1109/TPWRS.2016.2569563.

Mogharbel, B., Fan, L., and Miao, Z. (2015). Least squares estimation-based synchronous generator parameter estimation using PMU data. In *2015 IEEE Power Energy Society General Meeting*, 1–5. doi: 10.1109/PESGM.2015.7286559.

Perić, V.S. and Vanfretti, L. (2014). Power-System Ambient-Mode Estimation Considering Spectral Load Properties. *IEEE Transactions on Power Systems*, 29(3), 1133–1143. doi:10.1109/TPWRS.2013.2292331.

Saarinen, L., Norrlund, P., and Lundin, U. (2015). Field Measurements and System Identification of Three Frequency Controlling Hydropower Plants. *IEEE Transactions on Energy Conversion*, 30(3), 1061–1068. doi: 10.1109/TEC.2015.2425915.

Saarinen, L., Norrlund, P., Lundin, U., Agneholm, E., and Westberg, A. (2016). Full-scale test and modelling of the frequency control dynamics of the Nordic power system. In *2016 IEEE Power and Energy Society General Meeting (PESGM)*, 1–5. doi:10.1109/PESGM.2016.7741711.

Sigurd Hofsmo Jakobsen and Kjetil Uhlen (2017). Vector fitting for estimation of turbine governing system parameters. In *Powertech*.

Stott, B., Jardim, J., and Alsac, O. (2009). DC Power Flow Revisited. *IEEE Transactions on Power Systems*, 24(3), 1290–1300. doi:10.1109/TPWRS.2009.2021235.

Working Group on Prime Mover and Energy Supply Models for System Dynamic Performance Studies (1992). Hydraulic turbine and turbine control models for system dynamic studies. *IEEE Transactions on Power Systems*, 7(1), 167–179. doi:10.1109/59.141700.